WEENTECH Proceedings in Energy

GCESD 2015

24th -26th February 2015
Technology Park, Coventry University
Coventry, United Kingdom

Volume 1: Global Conference on Energy and Sustainable Development, May 2015

ISBN: 978-0-9932795-0-8

www.weentech.co.uk

Edited by: Dr. Ashish Shukla
Published by World Energy and Environment Technology Ltd.

Contents

Proceedings of the Global Conference on Energy and Sustainable Development
GCESD2015
February 24-26, 2015, Technology Park, Coventry University
Coventry, UK

STRATEGIES FOR SUSTAINABLE AND EFFICIENT ENERGY CONSUMPTION IN A REHABILITATION CLINIC IN SOUTHERN SPAIN

Alejandro Ayala
Dep. de Física Aplicada II
E.U. Politécnica.
Universidad de Málaga.
Louis Pasteur 35, Campus de Teatinos. 29071 Málaga, Spain

Llanos Mora-López
Dep de Lenguajes y Ciencias de la Computación ETSI Informática
Universidad de Málaga.
Campus de Teatinos.
29071 Málaga, Spain

Mariano Sidrach-de-Cardona
Dep. de Física Aplicada II
E.U. Politécnica.
Universidad de Málaga.
Louis Pasteur 35, Campus de Teatinos. 29071 Málaga, Spain
Email: msidrach@uma.es

ABSTRACT

This article presents the work carried out to implement the use of solar thermal energy in a rehabilitation clinic located in southern Spain. The objective is to reduce the consumption of fossil fuels and improve energy sustainability and efficiency of clinical current processes and contribute to a better use of the abundant solar resources in this area. We have developed a strategy that allows better utilization of production of solar collectors. In the first phase we have designed a solar thermal system for domestic hot water supply of 30 double rooms (half the current capacity of the center) and pool heating. This pool is outdoors, with a capacity of 160 m3 and is used for medical treatment during the months of May to September. The management of the use of water heated in the collectors during this period has been established to give priority to the pool heating and the use of the excess energy to supply the hot water system. We have simulated the system performance using the F-char method. The results show that the designed system is able to cover 100% of the energy needs of the pool and cover 60% of the hot water needs of the 30 rooms. It can be stated that the use of this type of energy in facilities such as the one described in this paper allows maximizing the thermal energy produced and represent a significant saving of fossil fuels.

INTRODUCTION

The work described in this paper was performed in clinical Montebello. It is a Danish public rehabilitation clinic, non-profit, located in southern Spain (Fig. 1). The facility was built in 1974 and is a rehabilitation clinic since 1980.

Fig.1. Location of the clinic

It is located in Benalmádena Pueblo, Malaga (Spain). The treatments are Physiotherapy and Ergonomics. The clinic consists of several administrative buildings, offices, bedrooms, kitchen, apartments and stores, among others, as shown in Fig. 2. The energy supply so far has been done with gas (for cooking), electricity (for lighting, air conditioning and appliances) and diesel (to produce hot water for a primary circuit supplying both water hot, appliances, existing radiators for heating the different units and pool heating).

Fig. 2. Buildings of the clinic

An important part of this energy consumption can be supplied by solar thermal energy, [1], [2]. These include the consumption of sanitary hot water, kitchen electrical appliances and heating swimming pool in which is done the treatment and prevention of injuries or pathologies.

This article presents the work carried out to implement the use of solar thermal energy in this rehabilitation clinic. The objective is to reduce the consumption of fossil fuels and improve energy sustainability and efficiency of clinical current processes and contribute to a better use of the abundant solar resources in this area.

NOMENCLATURE

$\bar{G}_{d,g}$: monthly average global daily irradiation values on a horizontal surface per unit area

$\bar{G}_{d,dif}$: monthly average diffuse daily irradiation values on a horizontal surface per unit area

$\bar{G}_{d,dif}$: monthly average beam daily irradiation values on a horizontal surface per unit area

$\overline{K}_{d,g}$: monthly average clearness index,

$\bar{G}_{d,0}$: monthly average daily extraterrestrial solar irradiation per unit area

$\overline{K}_{d,dif}$: monthly average diffuse fraction of solar radiation

f: fraction of monthly total load supplied by a solar energy system

X, Y: dimensionless parameters used by f-chart

A_c: collector area (m^2)

F'_R: collector heat exchanger efficiency factor

U_L: collector overall loss coefficient ($W/m^{2o}C$)

Δt: total number of seconds in month,

$\bar{T}_a$: monthly average ambient temperature (ºC)

T_{ref}: empirically derived reference temperature (100ºC),

L: monthly total heating load for space heating and hot water (J)

$\bar{H}_T$: monthly average daily radiation incident on collector surface per unit area (J/m^2)

N: days in month

$(\overline{\tau\alpha})$: monthly average transmittance-absorbance product

T_m: main water temperature

T_w: the minimum acceptable hot-water temperature

F_t: correction factor (for X) for liquid heating systems

F_s : storage size correction factor (for X)

X_c: value of X corrected using correction for liquid heating systems and correction for storage size.

METHDOLOGY

Estimation of solar irradiation on solar collectors

The energy will receive tilted and oriented solar thermal collectors has been estimated using as input data the monthly average daily irradiation values on a horizontal surface, $\bar{G}_{d,g}$. Each monthly value is decomposed into diffuse, $\bar{G}_{d,dif}$, and beam irradiation, $\bar{G}_{d,dif}$. Diffuse irradiation is obtained using the expression proposed by Page [3]:

$$\overline{K}_{d,dif} = 1 - 1.3\overline{K}_{d,g}$$

Where $\overline{K}_{d,g}$ is the clearness index, defined as $\overline{K}_{d,g} = \frac{\bar{G}_{d,g}}{\bar{G}_{d,0}}$, being $\bar{G}_{d,0}$ the monthly mean daily extraterrestrial solar irradiation, $\overline{K}_{d,dif}$ is the diffuse fraction, defined as $\overline{K}_{d,dif} = \frac{\bar{G}_{d,dif}}{\bar{G}_{d,g}}$..

The beam irradiation is obtained using the expression:

$$\bar{G}_{d,b} = \bar{G}_{d,g} - \bar{G}_{d,dif}$$

The hourly values of horizontal global irradiance are calculated using these values and the expressions proposed by Collares – Pereira & Rabl [4]. For estimating the energy in the surface collectors the three components models has been used: beam, diffuse and reflected. The beam component has been estimated using the trigonometric relationship; the diffuse component has been estimated using the anisotropic model of Hay-Davies [5]. Finally, reflected component has been estimated assuming an isotropic reflection. The daily values of global irradiation on collectors (oriented and tilted) have been estimated by adding these three components.

Design of system

The system has been designed using the f-chart method, [6] that provides a means for estimating the fraction f of a total heating load that will be supplied by solar energy for a given solar heating system. This fraction depends on two dimensionless parameters X and Y:

$$X = \frac{A_c F'_R U_L (T_{ref} - \bar{T}_a)\Delta t}{L}, \qquad Y = \frac{A_c F'_R (\overline{\tau\alpha}) \bar{H}_T N}{L}$$

Where A_c is the collector area (m^2), F'_R is the collector heat exchanger efficiency factor, U_L is the collector overall loss coefficient (W/m^{2o}C), Δt is the total number of seconds in month, $\bar{T}_a$ is the monthly average ambient temperature (ºC), T_{ref} is the empirically derived reference temperature (100ºC), L is the monthly total heating load for space heating and hot water (J), $\bar{H}_T$ is the monthly average daily radiation incident on collector surface per unit area (J/m^2), N are the days in month and $(\overline{\tau\alpha})$ is the monthly average transmittance-absorbance product. For liquid heating systems it is also necessary to define an additional correction on X using the main water temperature T_m and the minimum acceptable hot-water temperature T_w as both affect the performance of solar water heating systems:

$$F_t = \frac{11.6 + 11.18T_w + 3.86T_m - 2.32\bar{T}_a}{100 - \bar{T}_a}$$

Moreover, the performance of system is determined by multiplying the dimensionless X by a storage size correction factor F_s as the storage capacity per square meter of collector area is different from 75 (that is the standard for developed f-chart):

$$F_s = \left(\frac{actual\ storage\ capacity}{standard\ storage\ capacity}\right)^{-0.25}$$

Taking into account the two correction factor for X, the final value X_c is obtained using the following expression:

$$X_c = XF_tF_s$$

The fraction f of the monthly total load supplied by the solar thermal system is given by the expression, [6]:

$$f = 1.029Y - 0.065X_c - 0.245Y^2 + 0.0018X_c^2X^2 + 0.0215Y^3$$

System description

The system is divided into the following subsystems:

- Centralized solar production system (collectors)
- Exchange system
- Solar accumulation central system
- Hydraulic distribution system
- Support system for the production of hot water. This system consists of two diesel boilers that already exist in the system.

The solar thermal system designed consists of 64 thermal collectors of 2.32m^2, making a total area of 148.5 m^2 collection integrated into the roofs of several buildings (Fig. 3). These covers are inclined 10° relative to the horizontal and with an azimuth of 60 degrees east.

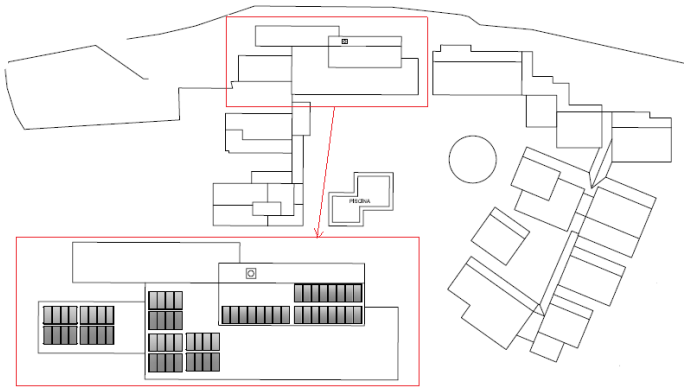

Fig. 3. Location of the solar thermal system.

The thermal energy collector provides two different storage subsystems, pool and domestic hot water, according to the strategy designed. A storage battery allows storing 5000l energy to maintain the temperature of the pool water for medical treatment between 31-33°C during daytime. A floating thermal blanket is used at night to prevent losses and optimize system performance. The hot water circuit also has another storage system with a total capacity of 3,500l.

The pool heating will be done through heat exchangers, either directly to the pool or through the storage tanks. For production of the domestic hot water, the exchange of heat from the storage tanks to the secondary energy will be done using an exchanger. Fig. 4 shows the entire system.

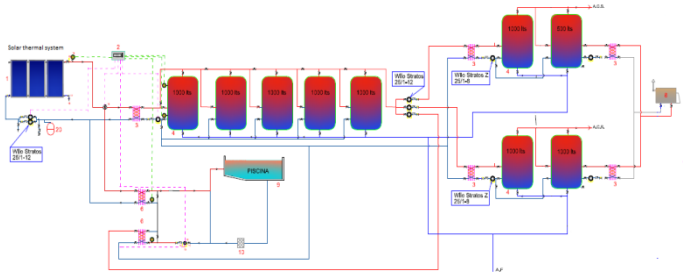

Fig. 4. Scheme of the system.

Proposed Strategy

The energy supplied by the collectors will be used to raise main water to the highest possible service level to be used for heating the pool. When this reaches its set point, the energy will be stored in the solar tank until the highest possible thermal level. The heated water in this storage tank will serve as feed to the solar energy water heater of each section of water which will take additional equipment fitted to raise its temperature, if necessary up to the preset temperature of consumption.

If necessary, the energy storage tanks can dump it to another exchanger circuit to provide the energy needed at this time.

RESULTS AND DISCUSSIONS

Solar energy availability

The installation is located in southern Spain that has high levels of irradiance throughout the year. Table 1 shows monthly mean daily values of solar global radiation on horizontal surface and on collectors surface, ambient temperature and water temperature.

	T_a	T_m	$\bar{G}_{d,g}$	$\bar{G}_{d,\alpha}$
Jan	12.1	8.0	9356	13405
Feb	12.8	9.0	12042	15481
Mar	14.0	11.0	16084	18641
Apr	15.8	13.0	19334	20208
May	18.7	14.0	23926	23408
Jun	22.1	15.0	25854	24476
Jul	24.7	16.0	26530	25431
Aug	25.3	15.0	24067	24474
Sep	23.1	14.0	18903	21075
Oct	19.1	13.0	14073	16082
Nov	15.1	11.0	10197	14199
Dec	12.6	8.0	8429	12430
Mean	18.0	12.3	17400	19109

Table 1. Ambient temperature (T_a), main water temperature (T_m), monthly mean horizontal solar global irradiation ($\bar{G}_{d,g}$, kJ/m^2/day) and global irradiation on surface collectors ($\bar{G}_{d,\alpha}$, kJ/m^2/day).

Analysis of consumptions

Swimming pool needs: the period of use of the pool is from May to September (inclusive). It should be at a temperature between 31 and 35 degrees. The hours of use are from 9:00 to 18:00, but in the months of May and September can be reduced by half hour (a first or last hour of operation), based on energy availability. To reduce power consumption, the pool is covered during the hours not used with a thermal blanket.

In order to optimize the thermal energy produced, it is expected that this energy will be used to supply domestic hot water for 30 rooms located in the same area that the solar thermal system and the kitchen when swimming pool is not used; these rooms are located in the same area where the solar installation will be installed.

The swimming pool loses heat by conduction to the ground, by convection to the air and by evaporation; a floating thermal blanket is used at night to prevent losses and optimize system performance. The energy requirements for the supply of hot water for 30 rooms have been estimated taking into account the difference between the main water temperature and the hot water temperature.

We have simulated the system performance using the F-char method using the data previously detailed. The results show that the designed system is able to cover 100% of the energy needs of the swimming pool and cover 60% of the hot water needs of the 30 rooms. It can be stated that the use of this type of energy in facilities such as the one described in this paper allows maximizing the thermal energy produced and represent a significant saving of fossil fuels.

CONCLUSIONS

We have developed a strategy that allows better utilization of production of solar collectors. This strategy will be implemented in several phases and includes the replacement and diversification of energy sources using solar energy systems as well as improving the thermal insulation of the building envelope.

In the first phase we have designed a solar thermal system for domestic hot water supply of 30 double rooms (half the current capacity of the center) and pool heating. This pool is outdoors, with a capacity of 160 m^3 and is used for medical treatment during the months of May to September. The management of the use of water heated in the collectors during this period has been established to give priority to the pool heating and the use of the excess energy to supply the hot water system. In the all other months of the year, when the pool is not used, the entire thermal system supplies the domestic hot water circuit.

ACKNOWLEDGMENTS

The authors acknowledge the assistance provided by the management team and staff of the clinic Institution Montebello.

REFERENCES

[1] E. Azad, Design, installation and operation of a solar thermal public bath in eastern Iran, Energy for sustainable development, 16(1), 68-73 (2012).

[2] Experimental-computational evaluation of a solar water heating system J.G.B. Saldana, P.Q. Diez, New and renewable energy technologies for sustainable development. International Conference on New and Renewable Energy Technologies for Sustainable Development, Ponta Delgada, Portugal, 405-418, Jun 24-26, 2002 (publication date, 2004).

[3] J. Page, The estimation of monthly values of daily total short wave radiation on vertical and inclined surfaces from

sunshine records for latitudes 40°N–40°S, Proc. UN Conf. New Sources Energy 4, 378–390 (1961).

[4] M. Collares-Pereira, A. Rabl, The average distribution of solar radiation-correlations between diffuse and hemispherical and between daily and hourly insolation values, Sol. Energy. 22, 155–164 (1979).

[5] J.E. Hay, Study of Shortwave Radiation on Non-horizontal Surfaces, Atmospheric Environ. Serv. Report No 79-12 (1979).

[6] J.A.Duffie and W.A. Beckman, Solar Engineering of Thermal Process. Wiley, third edition (2006).

Proceedings of the Global Conference on Energy and Sustainable Development
GCESD2015
February 24-26, 2015, Technology Park, Coventry University
Coventry, UK

ENERGY EFFICIENT CERAMIC ELECTROLYTE FUEL CELL SYSTEM WITH ENHANCED POWER DENSITY FOR IT-SOFC APPLICATION

R. Gupta
Department of Ceramic Engineering
Indian Institute of Technology (BHU), Varanasi
Varanasi, India
rohit.gupta.cer11@iitbhu.ac.in

Abstract—Remarkably high electrical efficiency at attractive economics can be achieved by using Ce0.8Gd1.2O1.2 (Gadolinium Doped Ceria (GDC)) as solid electrolyte in IT-SOFC (Intermediate Temperature-Solid Oxide Fuel Cell) and using La1-xSrxCo1-yFeyO3-δ (LSCF) as cathode where, $0 < x \leq 0.5$, $0 < y \leq 0.8$. Different solid oxide electrolyte samples were synthesized employing dry pressing technique, thereafter the samples were sintered at different temperatures ranging from 1350˚C to 1600˚C. Relative density as high as 93.93% was achieved for electrolyte samples. X-Ray Diffraction (XRD) pattern for sintered GDC samples reveals the presence of crystalline crystallographic system of cubic phases with crystal orientation such as (111), (200), (220), (311), (222), (400), (331), (420), thereby ensuring productive sintering. Impedance Analysis at different temperatures indicates that the ionic conductivity increases with the increase in sintering temperature and was found to attain its peak value at 1550℃. Exceptionally high power density of 347mW/cm2, 539mW/cm2 and 747mW/cm2 of 700℃, 750˚C and 800℃ were achieved indicating excellent electrolytic performance. This justified the competency of GDC to replace conventional YSZ (Yttrium Stabilized Zirconia) electrolyte. Further, different cathode samples were synthesized using combustion synthesis technique, thereafter the samples were sintered at different temperatures ranging from 1050˚C to 1150˚C for 4 hours in air. Single phase rhombohedral of LSCF is obtained and is confirmed by the peaks corresponding to (104), (110), (024), (300) and (306). Surface area of the sample having highest cobalt concentration is found to be much higher than other samples, that is, 14.579 m2/g. TG graphs shows that drastic weight loss occurs in three steps in the temperature range of 195-200℃, 300-340℃ and 430-460 ℃. Arrhenius plot suggests that DC conductivity increases with increase in densification for sample having lowest cobalt concentration while decreases in case of other samples, Of all the prepared samples, La0.54Sr0.4Co0.8Fe0.2O3±δ was found to be most efficient as it achieved current density as high as 2.12A/cm2 at 800℃ under cell operation voltage of 0.7 V. Hence the GDC electrolyte and LSCF cathode IT-SOFC fuel cell system can deliver attractive economics and consequently can be used for the production of clean energy allowing sustainable development.

Keywords—Gadolinium Doped Ceria, LSCF, Solid Oxide Fuel Cell, Electrochemical Performance, Impedance Analysis

INTRODUCTION

Due to the high energy conversion ratio, low pollution and fuel flexibility Solid oxide fuel cells (SOFCs) have attracted more and more attention in recent years [1-8].. It has significantly higher efficiency than that of conventional methods of power generation. Its fuel-to-electricity conversion efficiency is as high as 45-60%.

Solid oxide fuel cell (SOFC) is an all solid electrochemical device. Advantages of this class of fuel cells include high efficiency, long-term stability, fuel flexibility, low emissions, and relatively low cost etc. Due to its high class precedence over other conventional sources it has wide range of applications in different fields such as in space mission, transportation, aero planes, buildings, industrial remote areas, etc. One more reason for its edge over other conventional power sources is that it only produces heat and water as bi-product both of which can be used in one or other way.

The major challenge of SOFC developers is to reduce the operation temperature. The SOFC single cell consists of three major components: cathode, anode and electrolyte. The challenges encountered in the process of developing a better solid oxide fuel cell can be classified in two different classes- 1) challenges related to electrolyte, 2) challenges related to cathode. The first major challenge in development of electrolyte is its density, that is, the electrolyte must be dense enough to prevent the gas mixing. The ionic mobility of the electrolyte must have sufficient high ionic mobility because ions generated in cathodic side have to travel through the electrolyte. Also, the working temperature of the fuel cell must be as low as possible so that the maintenance cost and the heat up time could be reduced. For SOFC operating below 650℃ Doped ceria electrolytes, especially GDC electrolyte, are considered to be one of the most promising materials [9–11]. In case of high temperature Solid Oxide Fuel Cell, it needs to be protected by outer protective layers of ablative materials like OP-POSS/RF [12] and CS/RF [13]. Further, the two

electrodes should be porous enough to allow gas diffusion and surface area must be large so that more active sites would be available for ionisation of gases.

In SOFC, oxygen/air is generally used as oxidant gas which gets reduced to O2- at cathodic side. However, the kinetics of cathodic oxygen reduction reaction (ORR) is much slower than that of anodic reaction. The efficiency of SOFC is consequently controlled by the cathodic process. Reduction of oxygen in cathode layer takes place mainly at the triple phase boundaries (TPB) which in turn facilitate the electrochemical performance of the cell. Thus, kinetics of ORR can be made faster by increasing the TPB volume fraction. The cathode composition and microstructure markedly affect the TPB as well as the performance of the SOFC single cell. In this respect, mixed ionic and electronic conductor (MIEC) materials are efficient for IT-SOFC applications.

In the present study, attempt has been made to develop an electrolyte and a cathode composite materials for IT-SOFC applications. The material used in development of electrolyte is Gadolinium doped Ceria (GDC20) and Lanthanum Strontium Cobalt Ferrous (LSCF) composite was synthesized for cathode. Ceria based materials are an upcoming alternative solid electrolyte to compared yttria-stabilized zirconia (YSZ) in solid oxide fuel cell (SOFC) applications [14–16]. The effectiveness of an electrolyte is directly dependent on its ionic conductivity. This in turn depends on the mode of ionic transport within the ceramic lattice. In the case of GDC20, the main transport mechanism is through the oxide ion vacancies caused by the substitution of the Ce3+ ions by Gd4+ ions in the octahedral regions causing oxide ion vacancies by stoichiometric mismatch. This study is concerned with the effect of sintering temperature on the ionic conductivity by studying the properties of GDC20 samples sintered at the temperature 1350, 1400, 1450, 1550, 1600℃. The density of the samples is measured in PRECISA ES225SM-DR measurement device by measuring the weight in water and weight in air separately. Before measuring the ionic conductivity and the total resistance the sample has to be coated with platinum paste. To complete the coating procedure we have to use Hot Plate and then it has to be kept inside tubular furnace for 2 hours at 800℃. To measure the ionic conductivities, the samples had to be placed in an SI 1260 impedance/gain phase analyzer (32MHz to 100uHz range; DC current=0.0V; AC level=50mV; Sweep frequency= 5MHz to 1 Hz at 60 points/decade). The impedance readings are converted into resistance/reactance graphs and the grain, grain-boundary resistance or the total resistance are noted down from the graphs. Thermal etching is done to have the better image of the microstructure which can be get from SEM machine. Then SEM micrographs were taken in a Thermo-Electron Corporation field-emission SEM instrument to obtain the morphology of the sample.

Development of cathode composite materials based on La1-xSrxCo1-yFeyO3-δ (LSCF) where, $0 < x \leq 0.5$, $0 < y \leq 0.8$. First, three different compositions of LSCF powders (of varying concentration of cobalt and Iron), (CF-1), (CF-2), (CF-3) have been prepared using combustion synthesis technique (Table 1).

TABLE I. ABBREVIATION USED FOR CATHODE SPECIMENS

S. no.	Sample	Composition
1.	CF-1	La0.54Sr0.4Co0.8Fe0.2O3±δ
2.	CF-2	La0.54Sr0.4Co0.6Fe0.4O3±δ
3.	CF-3	La0.54Sr0.4Co0.5Fe0.5O3±δ

The precursor gels of the three compositions have been characterized by Thermal Gravimetric Analysis. Phase purity and structural characterization of the powder samples have been done by analysing X-Ray diffractograms. Surface area of the particles has been evaluated using BET isotherm. Then, three Composite cathode materials (CF-1A, CF-2A, CF-3A) have been prepared by sintering of LSCF powder at different temperature in temperature range 1050 to 1150℃. Densification studies of the composite cathode materials have been carried out within 1050-1150ºC. Electrical conductivity of the composite cathodes sintered at different temperatures have been measured in the temperature range 400–800℃ and correlated with the density of the sintered materials. The electrochemical performance of Ni-YSZ anode-supported SOFC having YSZ electrolyte with Co-CGO interlayer has been studied with the composite cathode (CF-1A) in the temperature range 700–800℃ using H2 as fuel and oxygen as oxidant. Highest current density of 2.12 A/cm^2 is achieved during testing at 800℃ measured at 0.7V.

EXPERIMENTATION

A. *Synthesis of GDC20 electrolyte*

99% pure cubic fluorite phased GDC20 powder was acquired from Cotter International, Mumbai and the analysis of powder size was done using DLS (Dynamic Light Scattering). GDC20 or pure GDC sample has molecular formula $Ce_{0.8}Gd_{0.2}O_{1.9}$. 10 gm of GDC20 was added with 0.2 gm of methyl cellulose, which acts as binder and the mixture is further added with 28 gm of alumina balls which is used for crushing the powders. Now 10 ml of isopropyl alcohol solution is added to the mixture as a solvent. The mixture was then ball milled for approximately 12 hours which results in formation of slurry. Now, the slurry was filtered from Al balls using sieve and the filtered slurry was taken in a beaker kept in an oven at 80℃ for almost 24 hours. Now, granulation of the dried powder was done using agate mortar. 0.5 gm of powder is taken and compaction was done using the 10 mm die and applying 3.5 tonnes per mm^2 of pressure using hydraulic pressing machine. The samples were then sintered using the Naberthem furnace for 2 hours and the sintering temperatures for each samples were 1350℃, 1400℃, 1450℃, 1550℃ and 1600℃. After Sintering the sample was kept inside a beaker containing water for boiling so that moisture present inside the pores was removed.

B. *Synthesis of LSCF cathode composite*

The synthesis procedure adopted for all the three compositions (CF-1, CF-2 and CF-3) is similar. The starting materials used for the synthesis are lanthanum (III) nitrate Hexahydrate (99%, SRL, India), strontium (II) nitrate (99%, s.d.fine, India), iron (III) nitrate Nonahydrate (Across Chemicals) and cobalt (II) nitrate Hexahydrate (99.5%, E. Merck, Germany) and L-alanine as a fuel (99%, E. Merck, India). First, a saturated aqueous solution of stoichiometric

amounts of the respective metal nitrates were mixed and stirred on a hot plate. Then required amount of alanine was added to these solution mixtures. After vigorous stirring, the whole solution was turned into a viscous gel. An instantaneous burning of those gels produces burnt ash. The ash-synthesized powders (ash) are then Calcined at 800˚C for four hours in air. The Calcined powder of each of the three different compositions was mixed with equal amount of phase pure Batch-A to make composite cathode materials. Then the resultant mixer was ball milled in an organic media to have homogeneity throughout the mixer. The composite cathode paste obtained was dried. Thereafter it was mixed with 0.05% of binder, to provide strength to the green body and the paste thus formed was taken for preparation of bar samples by pressing uniaxially with a specific pressure of 2 tonnes per mm^2. The green samples were sintered in the temperature range of 1050–1150℃ for 4 h in air.

RESULTS AND DISCUSSION (ELECTROLYTE)

C. Density measurement

Table 2 shows the variation of relative density against the sintering temperature. It reaches its maximum value at 1550℃, equal to 93.33%. This clearly shows that more the sintering temperature more is the densification but at higher temperature such as at 1600℃ the density observed is low due to the formation of non-uniform grains which happened because of more than one type of grain formation example bimodal formation.

TABLE II. THE VARIATION OF DENSITIES AMONG THE SINTERED SAMPLES ALONG WITH THE PERCENTAGE OF DENSITY AS COMPARED TO IDEAL VALUES.

Sintering Temperature	Experimental Density	% Relative Density
1350 °C	6.44gm/cc	87.3
1400 °C	6.50gm/cc	88.77
1450 °C	6.32gm/cc	89.95
1550 °C	6.80gm/cc	93.93
1600 °C	6.31gm/cc	87.1

D. XRD Analysis

XRD graph (Fig. 1) of all the samples yielded the same identical spectrum. Peaks were observed in the following crystal orientations: (111), (200), (220), (311), (222), (400), (331), and (420). It can be seen that the indices are either only even or odd but not a combination of both which suggests the presence of a cubic phase in the crystal lattice [18]. This results confirms the homogeneity starting raw material. Since no other peaks are visible it is seen that only cubic phase is present in the pressed and sintered samples.

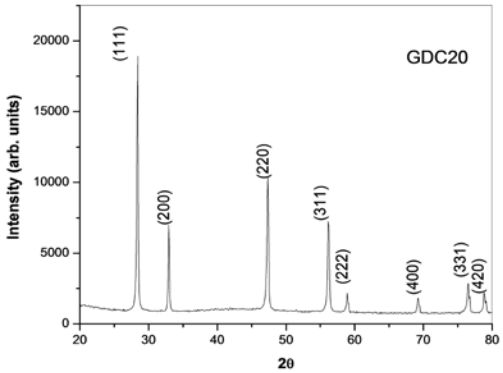

Fig. 1. XRD of sintered sample of GDC20

E. Microstructure Analysis

Scanning Electron Microscope images were taken for all the samples at magnifications of 3k, 5k, 8k, 10k and 20k at a constant electron voltage of 20 kV. In case of sample sintered at 1350℃, good densification was observed with density percentage of 88.95%. Grain growth can be seen clearly, in Fig. 2(a), with significant grain boundaries which were formed with rounded edges and only one type of grain growth was observed here and the mean grain size here was found to be 1.65 µm. In the case of sample sintered at 1400℃, images shows (Fig. 2(b)) density of the sample to be on better side as seen in the previous case, density percentage being 89.77. Grain formation was observed to increase as compared to the previous sintering temperature. Here also only one type of grain growth was observed and the mean grain size here was found to be 3.57 µm. In the case of sample sintered at 1550℃, images shows (Fig. 2(c)) less number of pores which ensures high density, density percentage being 93.93.

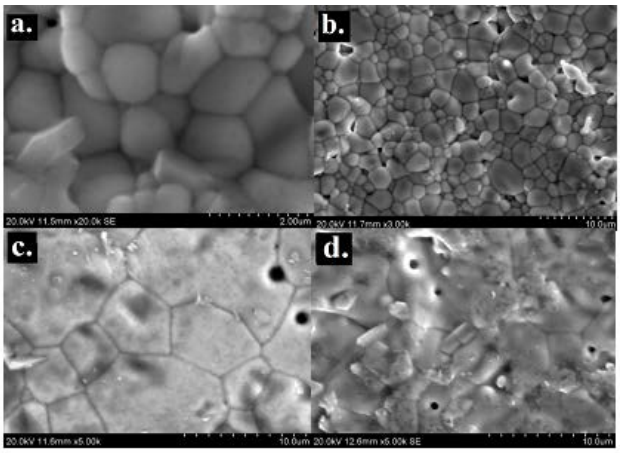

Fig. 2. SEM image of sample sintered at (a.) 1350℃, (b.) 1400℃, (c.) 1550℃, and (d.) 1600˚C

Pentagonal and hexagonal shape grains ascertained higher structural stability and grain formation was observed to increase as compared to the previous sintering temperature and here also only one type of grain growth was observed and the mean grain size here was found to be as high as 10.4 µm. In the case of sample sintered at 1600℃, large grains were observed along with bimodal formations, rod-like grains and flakes were formed which indicated that the grain growth

continued without retarding (Fig. 2(d)). The average grain size was found to be large, that is, 7.29 µm. Thus from this microstructure analysis it was confirmed that the optimum sintering temperature for GDC electrolyte is 1550℃.

F. Impedance Spectroscopy

Fig 3. shows the cole-cole plot of GDC20 sample sintered at 1550℃ for 2 hours (soaking time). The curve is resolved into semicircular arcs in high and mid frequency region with a straight line in low frequency region. The high freequency semicircle contributes to the grain conduction and mid frequency semicircle to grain boundary conduction. With increase in temperature, the diameter of semicircle is found to be decreasing which indicates that the resistance is decreasing with tempereture.

Conductivity was calculated from the total resistance of the sample at different temperatures and it is observed that with increase of temperature, conductivity is found to increase. The increase is significant in the high temperature region. At 800℃, the conductivity is 10 S/m, which is higher than the value of electrolyte reported earlier. The following plot shows the variation of conductivity with temperature.

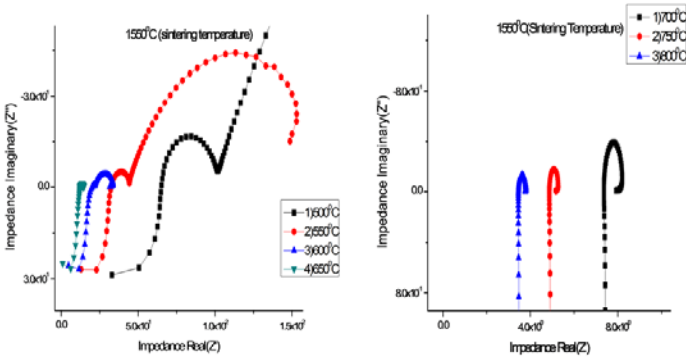

Fig. 3. Lower temperature range cole-cole plot of GDC20 sample sintered at 1550˚C

RESULTS AND DISCUSSION (CATHODE)

G. XRD Analysis

The Fig. 4 show the X-ray diffraction patterns for the samples CF-1, CF-2, CF-3 together suggesting that all were of same phase, which reveals that phase purity improves after calcination and single phase rhombohedral of LSCF was obtained. All the peaks had been identified with the standard JCPDS file number 490-284. The XRD data for the composites which have similar crystal structure with the CF series revealed that no new phase appear in the composite materials.

H. Surface Area

Table 3 shows the BET-surface area values of the samples CF-1, CF-2, CF-3 calcined powders. The resulted thus obtained that high surface area was obtained for sample haivng maximum cobalt compostion and minimum iron. Surface area, calculated using BET equation, of CF-1 powder was found to be as high as 14.579 m^2/g. Cathode with high surface area ensures high porosity and adequate gas diffusion which provides more active sites for ionisation of gases.

TABLE III. SURFACE AREAS OF CALCINED POWDER

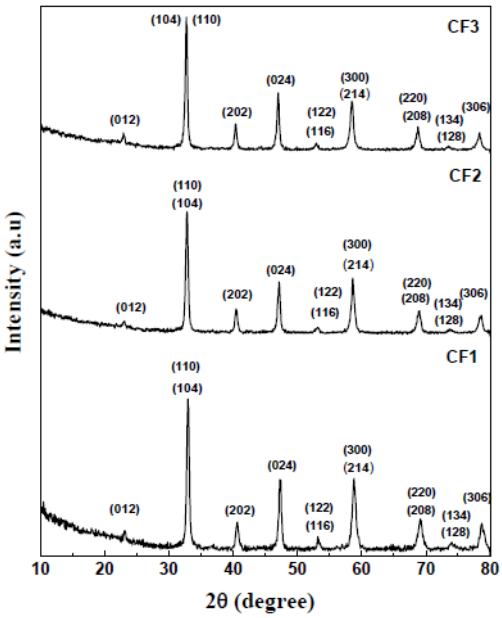

Fig. 4. XRD signature of sintered samples

I. DC Conductivity

All the synthesized cathodes, e.g., CF1A–CF-3A prepared under different sintering conditions are used for electrical conductivity measurement. Fig. 5 for samples CF-1A, CF-2A and CF-3, shows the Arrhenius plots $\ln(\sigma T)$ vs. $1/T$ indicating the influence of sintering temperature on the temperature-dependent electrical conductivity behaviour for the samples measured within the range between 400℃ and 800℃. Table 4. shows the value of data electrical conductivity. Also it is found that for sample CF-1A and CF-2A as sintering temperature increases, as densification increases, conductivity decreases. But for sample CF-3A, which has the lowest cobalt concentration of all the three samples, it is found that conductivity increases as densification increases.

TABLE IV. ELECTRICAL CONDUCTIVITY OF SINTERED SAMPLES

Sample name	Sintering Temperature (0C)	Conductivity (S/cm) at temperature				
		400	*500*	*600*	*700*	*800*
CF-1A	1050	673	683	652	574	478
	1100	536	550	535	489	413
	1150	516	541	530	481	409
CF-2A	1050	535	543	526	477	398
	1100	504	509	485	437	364
CF-3A	1050	330	330	321	295	251
	1100	421	428	420	393	341
	1150	507	526	518	484	411

The obtained results using Arrhenius equation are tabulated in the following tables. The data obtained are shown in table 5. Fig. 5 shows the Arrhenius plots of all the samples sintered at sintering temperature at which maximum conductivity was obtained for respective samples.

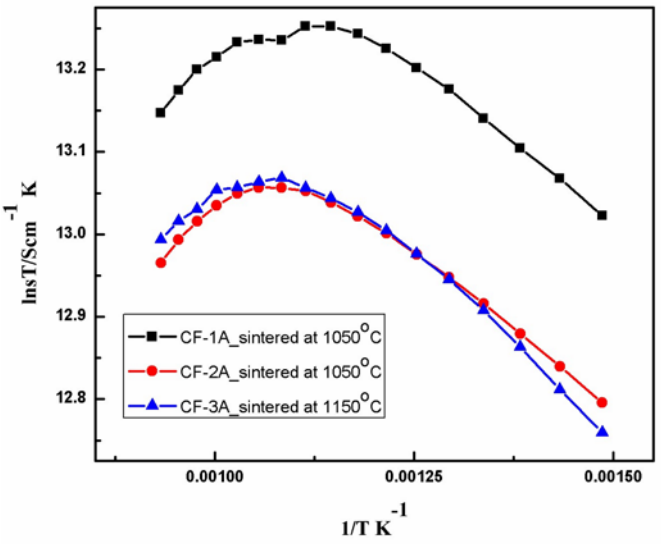

Fig. 5. Arrhenius plot of sample sintered at different temperatures

TABLE V. ACTIVATION ENERGY AT DIFFERENT TEMPERATURE RANGE.

Sample name	Sintering Temperature (^{0}C)	Activation Energy(10^{-5} eV)	
		High temperature	*Low Temperature*
CF-1A	1050	8.3436	8.3301
	1100	8.5853	7.879
	1150	8.3487	8.3350
CF-2A	1050	8.4296	7.4748
	1100	8.3608	7.4232
Cf-3A	1050	8.4554	7.6331
	1100	8.5156	7.3114
	1150	8.4735	6.9501

J. Electrochemical Performance

Fig. 6 shows electrochemical cell performance of the

S. no.	Sample	Surface area (m^2/g)
1.	CF 1	14.579
2.	CF 2	10.778
3.	CF 3	2.434

composite cathode sample CF-1A. In these cells, Co- CGO interlayer has been used. It can be seen that cell produces a current density as high as 2.12 A/cm^2, at 800℃ under cell operating voltage of 0.7V. Table 6 shows the variation of electrochemical properties with temperature for cathode composite sample CF-1A.

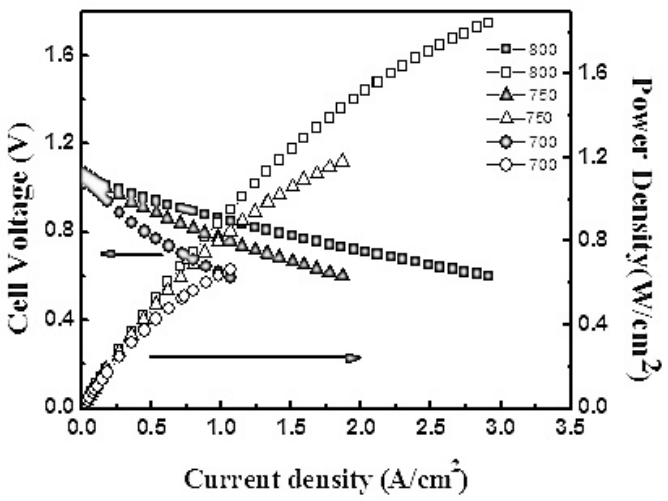

Fig. 6. Electrochemical cell performance of CF-1.

TABLE VI. VARIATION OF ELECTROCHEMICAL PROPERTIES OF CF-1

Electrochemical Property	Temperature(^{0}C)		
	800	*750*	*700*
Current Density(A/cm2)	2.11	1.33	0.729
Power Density(W/cm2)	1.47	0.936	0.510

COMPARISON WITH CONVENTIONAL SOURCES OF POWER

This work is an ceaseless effort in the direction coherence with technological advancement in the field of efficient eco-friendly non-conventional methods of power generation which promises to deliver attractive economies and yet at the same time it does so without much affecting the natural ecosystem and thus allowing sustainable development.

Solid Oxide Fuel Cell (SOFC) is an electrochemical cell and are very similar to conventional batteries which we use in our daily life. But unlike most batteries, which stop working when they use up their reactive materials, fuel cells can continuously make electricity if they have a constant fuel supply. SOFC can run on variety of eco-friendly fuels, including natural gas, biogas, hydrogen and air (for oxygen supply). SOFC creates electricity without much affecting the environment with efficiency as high as 60-70% whereas, the conventional sources affects the environment have ideal efficiency reaching up to only 40%. There is no harmful emissions in case of SOFC [19]. SOFC have high fuel to electricity conversion ratio and therefore they can provide better economies.

Apart from this, large systems generate more power than can be consumed in their immediate area, so a lot of their electricity has to be sent to other places through transmission lines. Unfortunately, some power is lost in the process. On the other hand, smaller systems like SOFC are physically smaller in size, so they can be placed closer to power users. And

depending upon the power requirement the different amount of SOFC stacks can be used at the place of use to fulfill the requirement. Thus, its efficiency and feasibility is further strengthened when factors like distribution and transmission of electricity are also taken into account. Further, its various salient features are compared with conventional sources of energy and are listed in table 7.

TABLE VII. COMPARISON OF FUEL CELL WITH CONVENTIONAL POWER SOURCES

Various salient features	**Fuel cell stack(SOFC)**	**Conventional power sources**
Process	Electrochemical reaction	Thermo dynamical process
Power transfer	Easy and economical as SOFC can be carried along	Neither easy nor economical
Eco-friendly	Yes	No
Fuel	Natural gas, Biogas, propane etc.	Conventional sources
Harmful Emission	No	Yes
Long-term stability	Yes	No
Fuel flexibility	Yea	No
By products	Heat and water	No such useful by product
Efficiency	Max 70%	Max 30%-40%
Power transmission loss	Negligible	Significant

CONCLUSION

GDC20 electrolytes were synthesized at different sintering temperatures. It is evident for the results that the relative density of 1550℃ sample was the highest and is hence the optimum sintering temperature. The ionic conductivity calculated in the temperature regime of 600-800℃ is higher than the reported value, indicating that GDC20 can be effectively used as an electrolyte for IT-SOFC application. Three different cathode powder were prepared by combustion synthesis. The LSCF-based cathode composite powders were prepared to investigate it for IT-SOFC application. Samples were compacted and were sintered at three different sintering temperature. Densification study and electrical conductivity were measured of all three cathode composite. It is found that for higher temperature range it shows metallic character and for lower temperature range it shows semi-conductor character. Electrochemical study of single cell using CF-1A ($La_{0.54}Sr_{0.4}Co_{0.8}Fe_{0.2}O_{3\pm\delta}$) composite cathode reveal its high efficiency for IT-SOFC application. The present study put forward the Solid Oxide Fuel Cell system which can be used as an efficient eco-friendly power source.

REFERENCES

[1] N.Q. Minh, “Ceramic fuel cells”, J Am Ceram Soc, vol. 76, pp. 563-588, 1993.

[2] B.C.H. Steele, “Materials for fuel cells”, Nature, vol. 414, pp. 345–352, 2001.

[3] M. Doriya, “SOFC system and technology”, Solid State Ionics, vol. 152/153, pp. 383–392, 2002.

[4] R. Bove, P. Lunghi and N. M.Sammes, “SOFC system and technology”, Int. J. Hydrogen Energ., vol. 30, pp. 189, 2005.

[5] W. Zhang, E. Croiset, P.L. Douglas, M.W. Fowler and E. Entchev, “SOFC system and technology”, Energy Convers. Manage., vol. 46, pp. 181, 2005.

[6] A. O. Omosun, A. Bauen, N. P. Brandon, C. S. Adjiman and D. Hart. J. “Power Sources”, vol. 131, pp. 96, 2004. 131(2004) 96.

[7] S. H. Chan and Z. T. Xia, “J. Electrochem. Soc”, vol. 148, pp. 388, 2001.

[8] F. Ishak, I. Dincer and C. Zamfirescu, “J. Power Sources”, vol. 212, pp. 73, 2012.

[9] B.C.H. Steele, “Appraisal of Ce1_yGdyO2_y/2 electrolytes for ITSOFC operation at 500_C”, Solid State Ionics, vol. 129, pp. 95-110, 2000.

[10] M. Mogensen, N.M. Sammes, G.S. Tompsett, “Physical, chemical and electrochemical properties of pure and doped ceria”, Solid State Ionics, vol. 129, pp. 63-94, 2000.

[11] J. Liu, B.D. Madsen, Z. Ji , S.A. Barnett, “A fuel-flexible ceramicbased anode for solid oxide fuel cells”, Electrochem Solid - State Lett, vol. 5, pp. A122-125, 2002.

[12] R. Gupta, Balasubramanian K., “Hybrid caged nanostructure of ablative composites of octaphenyl-POSS/RF as heat shields”, RSC Advances, vol. 5, pp. 8757-69, 2015.

[13] R.Gupta, Balasubramanian K., Y. Badhe, “Cost effective, low density, carbon soot doped resorcinol formaldehyde composite for ablative applications”, RSC Advances, vol. 5, pp. 23622-34, 2015.

[14] F. Snijkers, J.S.M. Ferreira, J. Luyten, “Aqueous tape casting of yittria stabilized zirconia using natural product binder”, J Eur Ceram Soc, vol. 24, pp. 1107-10, 2004.

[15] B.C.H. Steele, “Appraisal of Ce1−yGdyO2−y/2 electrolytes for IT-SOFC operation at 500 ◦C”, Solid State Ionics, vol. 129, pp. 95-110, 2000.

[16] D.L. Maricle, T.E. Swaar and S. Karavolis, “Solid State Ionics”, vol. 52, pp. 173-182, 1992.

[17] M. Godikemeiker, K. Sasaki and L. J. Gauckler, “Electrochemical characteristics of cathodes in solid oxide fuel cells based on ceria electrolytes”, J. Electrochem. Soc., vol. 144, pp. 1635-1646, 1997.

[18] R.D. Shannon, “Revised effective ionic radii in halides and chalcogenides”, Acta Crystallogr, vol. A32, pp. 751-767, 1976.

[19] “Data from The International Fuel Cells, a United Technology Company”, Fuel Cells Review, 2000.

Commonwealth Energy and Sustainable Development Network (CESD-Net)

CESD-Net is a major global initiative in energy and sustainable development. The objective of network is to promote energy and sustainable development in commonwealth countries.
Focussing on Multidisciplinary Research, Promoting Future Low Carbon Innovations, Transferring Knowledge and Stimulating Networking among Stakeholders to Ensure the UK Achieves World Leading Status in Energy and Sustainable Development. https://www.weentech.co.uk/cesd-net/

In today's world we strive to reduce carbon emissions and work towards energy efficiency and sustainable development. Sustainable development can only be achieved by efficient resource utilisation, generation and use of renewable energy and improving user awareness towards low carbon life style. Reducing energy demand through informed choices and user engagement is important in this context.

The "Global Conference on Energy and Sustainable Development-GCESD2015" highlighted progress that has been made around the globe towards energy efficiency, renewable energy, sustainability, resource utilisation and associate management and assessment methods. The presentations showed the depth and breadth of research across different research areas ranging from think film solar cells to sustainability issues in dams. It showed the real contributions and work going around the globe towards sustainable development. The conference has been a great success and we thank all our participants, organisers and committee members for their valuable contributions.

Editor: Dr. Ashish Shukla

Dr. Shukla is Senior Researcher at Coventry University, UK. He has more than ten years of research experience in the field of building engineering physics, energy management, energy generation within building envelopes and solar thermal engineering. Dr. Shukla has worked on various projects funded by the EPSRC, TSB, Welsh Assembly government, Low carbon research institute and Eon. He has strong expertise in thermal/mathematical modelling of energy systems, product design and development and computer simulations.

WEENTECH Proceedings in Energy
Global Conference on Energy and Sustainable Development 2015
www.weentech.co.uk

WEENTECH Proceedings in Energy- Global Conference on Energy and Sustainable Development 2015
Edited by: Dr. Ashish Shukla
Publisher: World Energy and Environment Technology Ltd., Coventry, United Kingdom
Publication date: 05 May 2015
Pages: 1-223
ISBN: 978-0-9932795-0-8
To purchase e-book online visit www.weentech.co.uk or email conference@weentech.co.uk